Inorganica Chimica Acta 516 (2021) 120119

Contents lists available at ScienceDirect

Inorganica Chimica Acta

journal homepage: www.elsevier.com/locate/ica

Research paper

Bimetallic and trimetallic chains of Fe-CN-Ln complexes: Synthesis, structural characterization, and magnetic properties

Yashu Liu [a,c], Chao Chen [b], Rongyao Dong [b], Kang Wu [b], Hongbo Zhou [b,c,*], Xiaoping Shen [b], Shaowei Chen [c]

[a] School of Environmental and Chemical Engineering, Jiangsu University of Science and Technology, Zhenjiang 212003, China
[b] School of Chemistry and Chemical Engineering, Jiangsu University, Zhenjiang 212013, China
[c] Department of Chemistry and Biochemistry, University of California, 1156 High Street, Santa Cruz, CA 95064, United States

A B S T R A C T

Two new one-dimensional cyanide-bridged complexes, [Gd (DMF)$_4$(H$_2$O)$_2${Fe(CN)$_6$}]·H$_2$O (1) and [{CuL}Gd(H$_2$O)$_3${Fe(CN)$_6$}]·3H$_2$O (2) (H$_2$L = N,N'-(2-Hydroxy-propane-1,3-diyl)bis(3-methoxysalicylaldiimine) were obtained in the attempt of constructing heterotrimetallic 3d-3d′-4f systems with these reaction precursors. Interestingly, the two complexes show rather comparable structures with a chain-like skeleton, although one features a typical bimetallic structure while the other behaves as a trimetallic system. To the best of our knowledge, the complexes are new in the Fe-CN-Ln family, which is especially suitable for magnetic study of the role of the third metal ions in the system. X-ray diffraction results clearly indicated the formation of the interesting chain structures of these complexes, which were further confirmed by magnetic investigation.

1. Introduction

The interesting structures and magnetic properties of molecular assemblies via a wide range of metal centers and designed organic ligands have been attracting extensive interest both from the fundamental and technological perspectives [1–7], due to their potential applications in diverse areas, such as high-density information storage, quantum computing, and molecular electronics [8,9]. Within this context, heterotrimetallic complexes represent a unique system [10–20]. The most effective ligands that can be used to synthesize heterotrimetallic complexes is the Salen-type Schiff base ligands [20], which can accommodate two different metal ions by taking advantage of the different coordination cavities without losing the ability to further react with other metal precursors. Interestingly, the obtained heterotrimetallic complexes derived from Salen-type ligands and hexacyanometalates show a flexible and ever-changing structure. With the similar substructural unit, they can behave as V-shaped trinuclear clusters [21–25], distorted quadrilateral hexanuclear clusters [26], linear hexanuclear clusters [21,24,25], 1-D chain [21,25,27,28] or 2-D networks [25]. From the point of magnetism, another benefit to study such complicated spin systems is that they can provide an ideal environment to investigate how the multiple pathways of magnetic exchanges contribute to the final magnetic properties, offering a valuable opportunity to understand and tune the magnetic exchanges so that a positive synergetic effect between the magnetic exchanges and single ion magnetic anisotropy can be achieved.

In this study, we construct heterotrimetallic systems by using a modified Salen-type ligand (Scheme 1) prepared with 1,3-diamino-2-propanol, because the tuning of the functional group often leads to a significant change of the structural arrangement. In addition, the added oxygen atom brought by 1,3-diamino-2-propanol could participate in the coordination [29,30], which may be essential in structural control of the spin systems. Unexpectedly, two new 1-D cyanide-bridged complexes, [Gd(DMF)$_4$(H$_2$O)$_2${Fe(CN)$_6$}]·H$_2$O (**1**) and [{CuL}Gd(H$_2$O)$_3${Fe(CN)$_6$}]·3H$_2$O (**2**) (H$_2$L = N,N'-(2-Hydroxy-propane-1,3-diyl)bis(3-methoxysalicylaldiimine) were obtained, which show comparable chain-like structures. Below we report the synthesis, structural characterization, and magnetic properties of the complexes.

2. Experimental section

2.1. Materials and physical measurements

The basic chemical reagents were all commercially available and used as received without further purification. N,N'-(2-hydroxy-propane-1,3-diyl)bis(3-methoxysalicylaldiimine copper (II)(CuL) were prepared according to the procedure reported previously [31]. Elemental analysis for C, H and N was conducted on a Perkin-Elmer 240C analyzer. Infrared

* Corresponding author.
E-mail address: zhouhb@ujs.edu.cn (H. Zhou).

https://doi.org/10.1016/j.ica.2020.120119
Received 9 August 2020; Received in revised form 4 October 2020; Accepted 1 November 2020
Available online 5 November 2020
0020-1693/

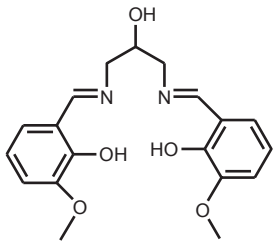

H_2L

Scheme 1. Salen-type ligand (H_2L) prepared with 1,3-diamino-2-propanol.

spectra were recorded on a Nicolet FT-170SX spectrometer. Magnetic susceptibility of the polycrystalline samples was measured on a Quantum Design MPMP-XL7 SQUID magnetometer, and the data was corrected according to the diamagnetism of the constituent atoms estimated from the Pascal constants [32].

2.2. Synthesis of $[Gd(DMF)_4(H_2O)_2\{Fe(CN)_6\}]\cdot H_2O$ (1)

A methanol solution (5 mL) of CuL (0.21 g, 0.5 mmol) was added into a methanol solution (5 mL) of $Gd(NO_3)_3\cdot 6H_2O$ (0.23 g, 0.5 mmol), and the mixture was stirred at room temperature for about 10 min, into which was then added an aqueous solution (5 mL) of $K_3Fe(CN)_6$ (0.16 g, 0.5 mmol) and 1 mL of DMF. The solution was left in the dark allowing slow evaporation without disturbance, such that yellow crystals were formed after one week, which were collected, washed with dimethyl ether and dried in a vacuum. Anal. found: C, 30.45; H, 4.65; N, 19.41%. Calcd for $C_{18}H_{34}FeGdN_{10}O_7$: C, 30.21; H, 4.78; N, 19.57%. IR: ν_{max}/cm^{-1} 3365 (vs), 2151 (m), 1652 (s), 1495(m), 1435 (s), 1381 (s), 1252 (m), 1112 (m), 1058 (w), 682 (w).

2.3. Synthesis of $[\{CuL\}Gd(H_2O)_3\{Fe(CN)_6\}]\cdot 3H_2O$ (2)

A methanol solution (5 mL) of CuL (0.21 g, 0.5 mmol) was added under stirring into a methanol solution (5 mL) of $Gd(NO_3)_3\cdot 6H_2O$ (0.23 g, 0.5 mmol). The mixture was then layered carefully onto an aqueous solution (5 mL) of $K_3Fe(CN)_6$ (0.16 g, 0.5 mmol) in a glass tube allowing the reaction precursors to diffuse slowly into each other. The solution was left without disturbance, and block green crystals were formed after several days, which were collected, washed with dimethyl ether, and dried in a vacuum. Anal. found: C, 33.52; H, 3.52; N, 12.63%. Calcd for $C_{25}H_{32}CuFeGdN_8O_{11}$: C, 33.47; H, 3.59; N, 12.49%. IR: ν_{max}/cm^{-1} 3282 (m), 2122 (s), 1621 (s), 1571 (m), 1470 (s), 1292 (m), 1232 (m), 1060 (m), 739 (w), 640 (m).

2.4. X- ray crystallography

The single-crystal XRD patterns of complexes **1** and **2** were collected at 173 K on a Bruker SMART-APEX-III diffractometer equipped with a graphite-monochromatic Mo K_α radiation ($\lambda = 0.71073$ Å) using the ω-scan mode. Diffraction data was calculated and reduced by XPREP, SMART and SAINT programs [33]. The structures was resolved based on direct methods and included in the refinement adopting a full-matrix least-squares method on F^2 with the SHELXL crystallographic software package [34]. All non-hydrogen atoms except solvent molecules were identified and included in the refinement with anisotropic thermal parameters, while some water oxygen atoms were refined isotropically, due to a slight disorder. Non-solvent hydrogen atoms were added by theoretical calculations, while most of the water hydrogen atoms were not located from the difference Fourier maps. CCDC 2008076 and 2008949 provide the supplementary crystallographic data for complexes **1** and **2**, respectively, which can be obtained free of charge from The Cambridge Crystallographic Data Centre via www.ccdc.cam.ac.uk/data_request/cif. The detailed crystal and structural refinement parameters are listed in Table 1.

3. Results and discussion

3.1. Syntheses and characterization

The synthesis of the complexes is based on a systematic attempt by fine-tuning the reaction conditions, such as the selection of precursors, solvent, and stoichiometric ratio of the reactants. Due to the complexity of the coordination reaction, in particular, when the ability of crystallization is taken into account, there is a considerable uncertainty in obtaining single crystals of the compounds. Among the recent series of complexes derived from the precursors of CuL, $Ln(NO_3)_3\cdot 6H_2O$ and hexacyanometalates, two synthetic routes yield positive results, in which the precursors were at least partially involved in the final complexes. Obviously, the moiety of CuL failed to be incorporated into complex **1**, while it was present in the molecular skeleton of **2**, indicating the strong effect of DMF that led to thermodynamic instability of the coordination interactions between the unit of CuL and Ln ions. It is worth noting that the comparable analogous structures can also been obtained under different reaction conditions, indicating these precursors could be flexibly constructed to certain structures in different reaction conditions [35–37]. The vibrational band around 2100 cm^{-1} is typical of the stretching vibration of the C≡N group, suggesting the presence of the cyanide group in the complexes [38].

3.2. Structural characterization

The selected structural parameters, such as bond lengths and angles, were shown in Table S1. The molecular diagrams of **1** and **2** including both the asymmetric unit and the complete chain structures are depicted in Fig. 1. Other structural diagrams are shown in Fig. S1 (Electronic Supplementary Information).

Complex **1** features a peculiar bimetallic 1-D square-wave chain-like structure, while **2** shows a trimetallic 1-D ladder-like arrangement. These structural characteristics were also found in some relevant analogous complexes derived from different metals and ligands with different synthesis procedures [35–37], indicating the thermodynamic

Table 1
Crystal data and structural refinement parameters for **1** and **2**.

	1	2
Formula	$C_{18}H_{34}FeGdN_{10}O_7$	$C_{25}H_{32}CuFeGdN_8O_{11}$
M/g·mol^{-1}	715.62	897.21
Crystal system	Monoclinic	Orthorhombic
Space group	$P2_1/n$	$P2_12_12_1$
a/Å	12.907(3)	13.047(3)
b/Å	12.632(3)	15.393(3)
c/Å	18.815(4)	16.893(3)
α/°	90	90
β/°	109.60(3)	90
γ/°	90	90
V/Å^3	2889.9(11)	3392.6(12)
Z	4	4
d_{calc}/g·cm^{-3}	1.640	1.731
F(000)	1424	1728
Collected reflections	25,396	31,595
Observed reflections	5615	6461
Independent reflections	5220	5725
R_{int}	0.0383	0.1173
Data/restraints/parameters	5615/0/342	6461/1/422
GOF[c] on F^2	1.065	1.023
R_1[a] ($I > 2\sigma(I)$)	0.0323	0.0829
wR_2[b] (all data)	0.0636	0.1810

[a] $R_1 = \sum||F_O|-|F_C||/\sum|F_O|$.
[b] $wR_2 = [\sum w(F_O^2-F_C^2)^2/\sum w(F_O^2)^2]^{1/2}$; $w = 1/\sigma^2(|F_O|)$.
[c] Goodness of fit: $GOF = [\sum w(F_O^2-F_C^2)^2/(n-p)]^{1/2}$, where n is the quantity of reflections and p is the quantity of parameters.

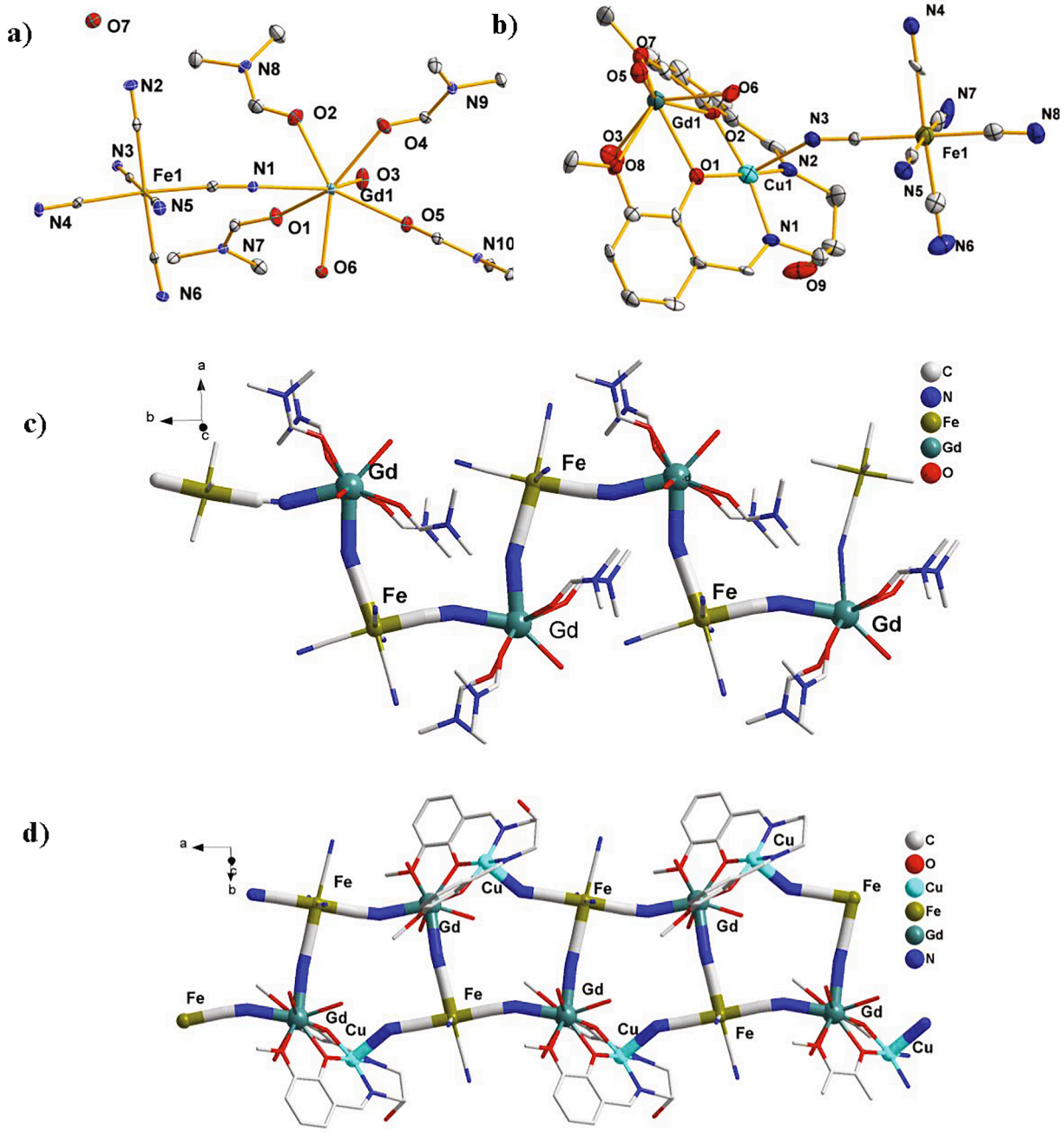

Fig. 1. Asymmetric unit of complexes **1** (a) and **2** (b) (ellipsoids set at the 30% probability level). 1-D chain structures of **1** (c) and **2** (d).

stability of these types of structures. As shown in Fig. 1a, the asymmetric unit of **1** consists of the moiety of one $[Fe(CN)_6]$ and one gadolinium(III) ion. The $[Fe(CN)_6]$ moiety is linked to two adjacent gadolinium(III) ions (one of the two gadolinium(III) ions is generated by a symmetric operation: 0.5-x, 0.5 + y, 0.5-z) in *cis*-mode using its two cyanide groups with all the remaining four cyanide groups terminal. The gadolinium(III) ion is eight-coordinated, forming a distorted dodecahedron configuration, where four of the sites were occupied by DMF molecules, and the remaining four positions were coordinated with two cyanide nitrogen atoms and two free water molecules. The key bond distance of Gd-$N_{cyanide}$ is 2.513(3) −2.519(3) Å, while the bond angle of Gd-$N_{cyanide}$-C is 159.5(3)°-162.3(3)°, which are in the typical range expected for such lanthanide ion based coordination complexes [20,39]. Eventually, the alternate connection of the $[Fe(CN)_6]$ unit and gadolinium(III) ion in *cis*-mode leads to the formation of 1-D square-wave chain-like structure (Fig. 1c).

Different from complex **1**, complex **2** can be described as a trimetallic 1-D ladder-like chain, similar structures have also been found in analogous complexes with different employed functional groups [40]. Interestingly, this kind of chains could be considered as the further decoration of the 1-D square-wave chain of **1** by filling the vacancy with additional copper ion. As shown in Fig. 1b, the asymmetric unit is composed of one $[Fe(CN)_6]$, one gadolinium(III) ion and one {CuL} moiety. The $[Fe(CN)_6]$ used its two *cis*-cyanide group to coordinate to gadolinium(III) ion, forming the square-wave chain-like skeleton, then additional coordination between gadolinium(III) ion and {CuL} via the phenoxo bridge as well as $[Fe(CN)_6]$ and {CuL}through the cyanide bridge results in the formation of 1-D ladder-like chains. The coordination mode of $[Fe(CN)_6]$ in **2** is comparable to that in **1** except that it uses its additional cyanide groups to connect the copper ion (the bond length of Cu-$N_{cyanide}$ = 2.419(15) Å, ∠Cu-$N_{cyanide}$-C = 142.2(13)°). The gadolinium(III) ion in **2** is nine-coordinated, which is different from the

coordination mode found in **1**, but comparable to the heterotrimetallic 2-D Cu-Gd-Fe complexes reported previously [25]. The bond distance of Gd-$N_{cyanide}$ is in the range of 2.483(17)–2.524(18) Å, while the bond angle of Gd-$N_{cyanide}$-C is 161.7(17)–170.0(17)°, which is comparable to parameters found in **1**. Finally, the metals formed a distorted pentagon {FeGdFeCuGd}, which further builds the 1-D ladder-like chain by sharing the Fe-Gd edges (Fig. 1d).

3.3. Magnetic properties

The magnetic properties of **1** and **2** were measured to help understand the magnetic coupling between the spin carriers in such structural environments. As shown in Fig. 2a, the room temperature values of $\chi_M T$ (χ_M refers to molar susceptibility) of **1** and **2** were 8.92 and 9.23 cm^3 K mol^{-1}, respectively, which is close to the spin-only values (8.23 cm^3 K mol^{-1} for **1** and 8.61 cm^3 K $mol^{-1}$for **2**) calculated for the spin dilute system $\{\chi_M T = N\mu_B^2 g^2[S_{Gd}(S_{Gd}+1)+S_{Fe}(S_{Fe}+1)+S_{Cu}(S_{Cu}+1)]/3k_B$ ($S_{Gd}=7/2$, $S_{Fe}=1/2$, $S_{Cu}=1/2$, $g=2$)}. As the temperature decreased, the $\chi_M T$ values of both **1** and **2** remained almost constant until 50 K. Then, a slight increase of the value upon cooling was detected for **2**, reaching the maximum value of 9.82 cm^3 K mol^{-1} at 14 K. No such increase of the $\chi_M T$ value was observed for **1**. After further cooling, both of the $\chi_M T$ values of **1** and **2** drop rapidly to the values of 7.85 and 8.69 cm^3 K mol^{-1} at 1.8 K, respectively.

The structural analysis revealed that complex **1** could be described as the 1-D infinite regular Fe-Gd bimetallic chain, which can be treated by Seiden approach [41] considering **1** as alternating chains of quantum spins $s=1/2$ and classical spins $S=7/2$. The intrachain Fe-CN-Gd magnetic coupling (J) could be modeled based on the following Hamiltonian H (with $S_{Gd,i}=S_{Gd,i+1}=7/2$ and $s_{Fe,i}=1/2$) considering the intermolecular interactions zj':

$$H = -J\sum_{-\infty}^{+\infty}(S_{Gd,i}s_{Fe,i}+s_{Fe,i}S_{Gd,i+1}) \quad (1)$$

$$\chi = \frac{\chi_{GdFe}}{1-[2zj'/(Ng^2\mu_B^2)]\chi_{GdFe}} \quad (2)$$

where the N, g, μ_B and χ are Avogadro constant, Lande factor, Bohr magneton and molar susceptibility, respectively.

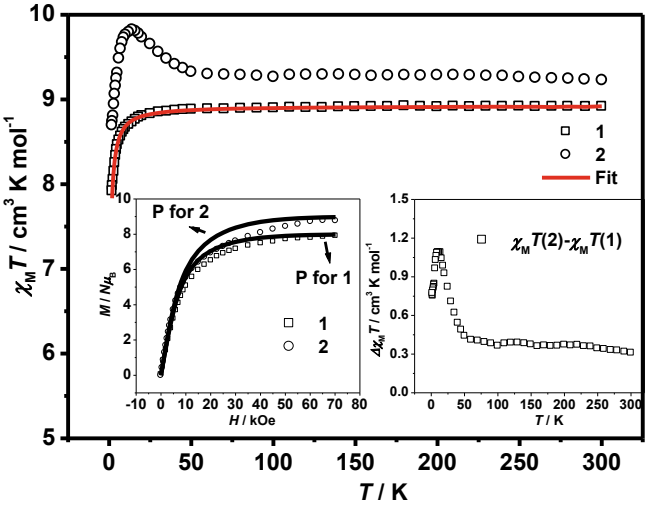

Fig. 2. Temperature dependence of $\chi_M T$ for complexes **1** and **2** measured at 0.1 kOe (the red solid line represents the best fit described in the text); Inset: Left is the field dependence of the magnetization for **1** and **2** measured at 1.8 K (the black solid lines marked P are the theoretical Brillouin curves for the paramagnetic FeGd and FeCuGd systems); Right is the $\Delta\chi_M T$ vs T plot calculated by subtracting the $\chi_M T$ value of **1** from **2.** (For interpretation of the references to colour in this figure legend, the reader is referred to the web version of this article.)

The experimental data of **1** could be well simulated at $J=-0.11$ cm^{-1}, $g=2.08$, $zj'=-0.01$ cm^{-1}. The fitting result indicates very weak aniferromagnetic interactions in complex **1**, which is in accord with results found in analogous complexes [25,42].

As for **2**, the peculiar trimetallic 1-D ladder-like chain structure makes it impossible to establish a reasonable model to simulate the magnetic behavior. However, an empirical approach can be used to analyze the magnetic interactions by comparing the magnetic behavior of **1** and **2** [43,44]. Considering that complex **2** can be viewed as the further decoration of the 1-D square-wave chain of **1** by filling the vacancy with additional copper ion. The difference between the $\chi_M T$ values of **1** and **2** can reveal the magnetic coupling nature in these complexes. As shown in the inset (right) to Fig. 2, the $\Delta\chi_M T$ value ($\Delta\chi_M T$ is defined as the difference between the $\chi_M T$ value of **1** and **2**) increases gradually upon cooling and more rapidly below 50 K and reaches the maximum value of 1.1 cm^3 K mol^{-1} at 12 K, such a behavior is indicative of ferromagnetic interactions, which can be attributed to the Gd-Cu coupling via the phenoxo bridge. Actually, the Gd-Cu coupling via the phenoxo bridge have been often found to be ferromagnetic in relevant complexes [43]. The rapid decrease of the $\Delta\chi_M T$ value below 10 K indicates the contribution from interchain antiferromagnetic interactions.

To further investigate the magnetic behavior, the field dependent magnetization was measured up to 70 kOe at 1.8 K, and the result clearly reveals that the response mostly coincide with the paramagnetic Brillouin curves [45] expected for a paramagnetic Fe-Cu-Gd system, indicating weak magnetic coupling between the spin carriers and lack of magnetic anisotropy, which is consistent with the above magnetic susceptibility analysis and the fact that gadolinium(III) ion is magnetically isotropic. From these analyses, it can be clearly understood that the weak interchain antiferromagnetic Fe-CN-Gd interactions are dominated by the ferromagnetic $Cu(O)_2Gd$ coupling, which contributes to the increase of the $\chi_M T$ value for **2** around 14 K. Finally, the weak interchain antiferromagnetic interactions lead to the rapid decrease of the value at very low temperature.

From the above structural and magnetic studies, we can see clearly the changes of the magnetic behavior brought by the third inserted copper ion. The literature reported examples related to the magnetic coupling via pathway of Cu…Gd, Fe…Gd and Fe…Cu are always found to be ferromagnetic, weak antiferromagnetic and uncoupled, respectively. (Table 2). Therefore, it is interesting to get the structural moieties of Fe…Gd out from the heterotrimetallic Fe…Gd…Cu entity here and understand more clearly of the magnetic behaviors of such complicated systems. In these complexes, the much stronger ferromagnetic Cu…Gd coupling dominates all the weaker antiferromagnetic contribution from Fe…Gd coupling, and plus the uncoupled Fe…Cu interactions. Indeed, the introducing of paramagnetic Cu^{II} ion into the structural skeleton of complex **1** has significantly changed the magnetic nature from paramagnetic-like to ferromagnetic type.

4. Conclusion

In summary, two new 1-D cyanide-bridged complexes based on Fe-Gd and Fe-Gd-Cu systems were synthesized and studied structurally and magnetically. Interestingly, the two complexes show structural similarity though one is bimetallic while the other is trimetallic, providing good examples to investigate the magnetic response when a third paramagnetic metal ion is brought into the bimetallic magnetic complexes without a significant change of the structural skeleton. Though the magnetic coupling was proved to be weak in complexes **1** and **2**, the influence of the structural changes on magnetic properties cannot be neglected, especially when the various different types of magnetic exchanges are taken into account to regulate the structures, leading to improved enhanced magnetic properties.

Table 2
Comparison of complexes **1** and **2** with reported analogous complexes.[a]

Complexes	Structure	Magnetic coupling Nature of Cu…Gd	Magnetic coupling Nature of Fe…Gd	Magnetic coupling Nature of Fe…Cu	Ref.
$[Gd(DMF)_4(H_2O)_2\{Fe(CN)_6\}]\cdot H_2O$	1-D	–	AF[b]	–	This work
$[\{CuL^1\}Gd(H_2O)_3\{Fe(CN)_6\}]\cdot 3H_2O$	1-D	F[b]	AF	–	This work
$[CuL^2]_2Ln(H_2O)_2Fe(CN)_6 7H_2O$	1-D chain	F	AF	F	15
CuL^3Fe_2Gd	1-D chain	F	AF	–	19
CuL^4Fe_2Gd	0-D cluster	F	–	–	10
$Cu_2L^5Fe_2Gd_2$	0-D cluster	F	AF	–	24
$[\{L^5Cu\}Gd(H_2O)_3\{Fe(CN)_6\}]_2 6H_2O$	0-D cluster	F	AF	–	26a
$[Cu(H_2L^5)(CH_3OH)]_2Gd(DMF)$-Fe $(CN)_6 2H_2O DMF$	0-D cluster	F	–	F	26b
$[\{L^5Cu(H_2O)\}Ln(MeOH)(H_2O)_2\{(\mu\text{-}CN)_2Fe(CN)_4\}]2H_2O$	1-D chain	F	AF	–	26c
$[Cu_2Gd(L^6)_2(H_2O)_4][Fe(CN)_6]\cdot 6H_2O$	1-D chain	F	–	–	26d
$[\{CuL^3\}Gd(H_2O)_3\{Fe(CN)6\}]\cdot 4H_2O$	1-D chain	F	AF	–	40
CuL^3FeGd	0D/1D	F	–	AF	22

[a] Abbreviations for the ligands: L^1 = N,N'-(2-Hydroxy-propane-1,3-diyl)bis(3-methoxysalicylaldiimine); L^2 = dianion of 1,4,8,11-tetraazacyclotradecane-2,3-dione; L^3 = 1,3-propanediyl-bis(2-iminomethylene-6-methoxyphenol)); L^4 = N,N'-(1,2-cyclohexanediylethylene)bis(salicylideneiminato) dianion; L^5 = N,N′-ethylenebis(3-methoxy salicylideneiminato) dianion; L^6 = 2,6-Bis(aceto-acetyl)pyridine.
[b] Abbreviations for the F and AF: F: ferromagnetic coupling; AF: Antiferromagnetic coupling.

Declaration of Competing Interest

The authors declare that they have no known competing financial interests or personal relationships that could have appeared to influence the work reported in this paper.

Acknowledgements

We are grateful for financial support from the National Nature Science Foundation of China (No. 21201084; 41601304), the Jiangsu Overseas Visiting Scholar Program for University Prominent Young & Middle-aged Teachers and Presidents, and the Jiangsu Government Scholarship for Oversea Studies (No. JS-2019-202).

Appendix A. Supplementary data

Supplementary data to this article can be found online at https://doi.org/10.1016/j.ica.2020.120119.

References

[1] J. Zhang, J. Ensling, V. Ksenofontov, P. Gutlich, A.J. Epstein, J.S. Miller, Angew. Chem. Int. Ed. 37 (1998) 657–660.
[2] M. Verdaguer, A. Bleuzen, V. Marvaud, J. Vaissermann, M. Seuleiman, C. Desplanches, A. Scuiller, C. Train, R. Garde, G. Gelly, C. Lomenech, I. Rosenman, P. Veillet, C. Cartier, F. Villain, Coord. Chem. Rev. 190 (1999) 1023–1047.
[3] J.S. Miller, D. Gatteschi, Chem. Soc. Rev. 40 (2011) 3065–3066.
[4] K.C. Mondal, A. Sundt, Y.H. Lan, G.E. Kostakis, O. Waldmann, L. Ungur, L. F. Chibotaru, C.E. Anson, A.K. Powell, Angew. Chem. Int. Ed. 51 (2012) 7550–7554.
[5] T. Kajiwara, Angew. Chem. Int. Ed. 56 (2017) 11306–11308.
[6] J.H. Jia, Q.W. Li, Y.C. Chen, J.L. Liu, M.L. Tong, Coord. Chem. Rev. 378 (2019) 2–381.
[7] Y.J. Ma, J.X. Hu, S.D. Han, J. Pan, J.H. Li, G.M. Wang, J. Am. Chem. Soc. 142 (2020) 2682–2689.
[8] M. Mannini, F. Pineider, C. Danieli, F. Totti, L. Sorace, P. Sainctavit, M.A. Arrio, E. Otero, L. Joly, J.C. Cezar, A. Cornia, R. Sessoli, Nature 468 (2010) 417–421.
[9] M. Mannini, F. Pineider, P. Sainctavit, C. Danieli, E. Otero, C. Sciancalepore, A. M. Talarico, M.A. Arrio, A. Cornia, D. Gatteschi, R. Sessoli, Nature Mater. 8 (2009) 194–197.
[10] X.W. Deng, L.Z. Cai, Z.X. Zhu, F. Gao, Y.L. Zhou, M.X. Yao, New J. Chem. 41 (2017) 5988–5994.
[11] E.J. Schelter, J.M. Veauthier, J.D. Thompson, B.L. Scott, K.D. John, D.E. Morris, J. L. Kiplinger, J. Am. Chem. Soc. 128 (2006) 2198–2199.
[12] D. Visinescu, J.P. Sutter, C. Ruiz-Perez, M. Andruh, Inorg. Chim. Acta 359 (2006) 7–440.
[13] M.A. Palacios, A.J. Mota, J. Ruiz, M.M. Hanninen, R. Sillanpaa, E. Colacio, Inorg. Chem. 51 (2012) 7010–7012.
[14] J. Martinez-Lillo, F.S. Delgado, C. Ruiz-Perez, F. Lloret, M. Julve, J. Faus, Inorg. Chem. 46 (2007) 3523–3530.
[15] H.Z. Kou, B.C. Zhou, R.J. Wang, Inorg. Chem. 42 (2003) 7658–7665.
[16] M.G. Alexandru, D. Visinescu, S. Shova, M. Andruh, F. Lloret, M. Julve, Inorg. Chem. 56 (2017) 2258–2269.
[17] H.B. Zhou, K. Wu, C. Chen, R.Y. Dong, Y.S. Liu, X.P. Shen, Eur. J. Inorg. Chem. (2017) 3946–3952.
[18] H.L. Wang, L.F. Zhang, Z.H. Ni, W.F. Zhong, L.J. Tian, J.Z. Jiang, Synthesis Cryst. Growth Des. 10 (2010) 4231–4234.
[19] M.G. Alexandru, D. Visinescu, M. Andruh, N. Marino, D. Armentano, J. Cano, F. Lloret, M. Julve, Chem. Eur. J. 21 (2015) 5429–5446.
[20] M. Andruh, Chem. Commun. 54 (2018) 3559–3577.
[21] N. Bridonneau, G. Gontard, V. Marvaud, Dalton Trans. 44 (2015) 5170–5178.
[22] M.J. Liu, K.Q. Hu, C.M. Liu, A.L. Cui, H.Z. Kou, New J. Chem. 40 (2016) 8643–8649.
[23] H.B. Zhou, C. Chen, Y.S. Liu, X.P. Shen, Inorg. Chim. Acta 437 (2015) 188–194.
[24] H.B. Zhou, C. Chen, J.W. Lu, Y.S. Liu, X.P. Shen, Inorg. Chim. Acta 453 (2016) 482–487.
[25] H.B. Zhou, C. Chen, K. Wu, Y.S. Liu, X.P. Shen, Eur. J. Inorg. Chem. (2016) 4921–4927.
[26] (a) T. Gao, P.F. Yan, G.M. Li, J.W. Zhang, W.B. Sun, M. Suda, Y. Einaga, Solid State Sci. 12 (2010) 597–604;
(b) K.Q. Hu, S.Q. Wu, A.L. Cui, H.Z. Kou, Trans. Met. Chem. 39 (2014) 713–718;
(c) W.B. Sun, P.F. Yan, G.M. Li, J.W. Zhang, T. Gao, M. Suda, Y. Einaga, Inorg. Chem. Commun. 13 (2012) 171–174;
(d) T. Shiga, A. Mishima, K. Sugimoto, H. Okawa, H. Oshio, M. Ohba, Eur. J. Inorg. Chem. 2012 (2010) 2784–2791.
[27] R. Gheorghe, A.M. Madalan, J.P. Costes, W. Wernsdorfer, M. Andruh, Dalton Trans. 39 (2010) 4734–4736.
[28] D. Visinescu, A.M. Madalan, M. Andruh, C. Duhayon, J.P. Sutter, L. Ungur, W. Van den Heuvel, L.F. Chibotaru, Chem. Eur. J. 15 (2009) (1814) 11808–11811.
[29] V. Chandrasekhar, A. Dey, S. Das, M. Rouzieres, R. Clerac, Inorg. Chem. 52 (2013) 2588–2598.
[30] A. Dey, S. Das, S. Kundu, A. Mondal, M. Rouzieres, C. Mathoniere, R. Clerac, R. S. Narayanan, Inorg. Chem. 56 (2017) 14612–14623.
[31] N. Kitajima, K. Whang, Y. Morooka, A. Uchida, Y. Sasada, J. Chem. Soc., Chem. Commun. (1986) 1504–1505.
[32] O. Kahn, Molecular Magnetism, Wiley-VCH, Weinheim, 1993.
[33] S.M.A.R.T. Bruker, SAINT and XPREP Area Detector Control and Data Integration and Reduction Software, Bruker Analytical X ray, Instruments Inc., Madison, Wisconsin, USA, 1995.
[34] G.M. Sheldrick, SHELXL-97, University of Gottingen, Germany, Program for the Refinement of Crystal Structure, 1997.
[35] A. Figuerola, C. Diaz, M.S. El Fallah, J. Ribas, M. Maestro, J.E. Mahia, Chem. Commun. (2001) 1204–1205.
[36] T. Lazarides, G.M. Davies, H. Adams, C. Sabatini, F. Barigelletti, A. Barbieri, S.J. A. Pope, S. Faulkner, M.D. Ward, Photochem. Photobiol. Sci. 6 (2007) 1152–1157.
[37] C.H. Ge, H.Z. Kou, Z.H. Ni, Y.B. Jiang, L.F. Zhang, A.L. Cui, O. Sato, Chem. Lett. 34 (2005) 1280–1281.
[38] K. Nakamoto, Infrared and Raman Spectra of Inorganic and Coordination Compounds, 4th ed., Wiley-Interscience, New York, 1978.

[39] H.L.C. Feltham, S. Brooker, Coord. Chem. Rev. 276 (2014) 1–33.
[40] R. Gheorghe, M. Andruh, J.P. Costes, B. Donnadieu, Chem. Commun. (2003) 2778–2779.
[41] J. Seiden, J. Phys. Lett. 44 (1983) L947.
[42] A. Figuerola, C. Diaz, J. Ribas, V. Tangoulis, J. Granell, F. Lloret, J. Mahia, M. Maestro, Inorg. Chem. 42 (2003) 641–649.
[43] A. Jana, S. Majumder, L. Carrella, M. Nayak, T. Weyhermueller, S. Dutta, D. Schollmeyer, E. Rentschler, R. Koner, S. Mohanta, Inorg. Chem. 49 (2010) 9012–9025.
[44] R. Koner, H.H. Lin, H.H. Wei, S. Mohanta, Inorg. Chem. 44 (2005) 3524–3536.
[45] M.I. Darby, Br. J. Appl. Phys. 18 (1967) 1415–1417.